Supplement of Geosci. Model Dev., 19, 4797–4815, 2026
https://doi.org/10.5194/gmd-19-4797-2026-supplement

Geoscientific Model Development
Open Access
EGU

Supplement of

Ammonia bidirectional flux model tailored for satellite retrieval parameter inversions

Michael Sitwell et al.

Correspondence to: Michael Sitwell (michael.sitwell@ec.gc.ca)

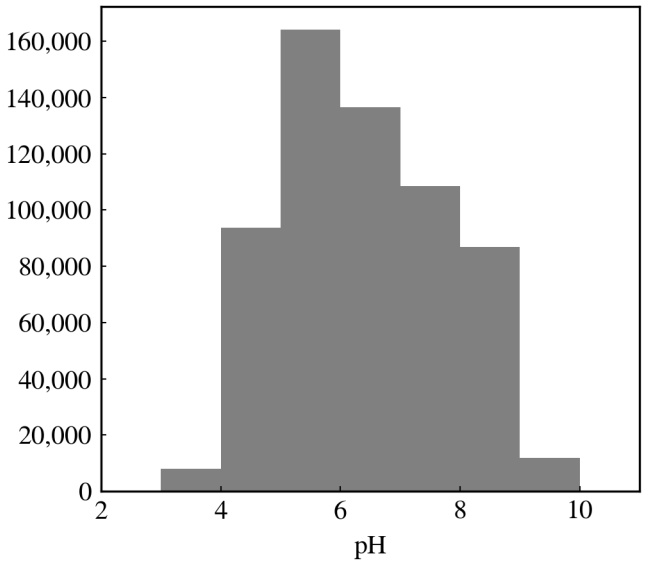

Figure S1. Soil pH values from the 2019 compilation of WoSIS soil database.

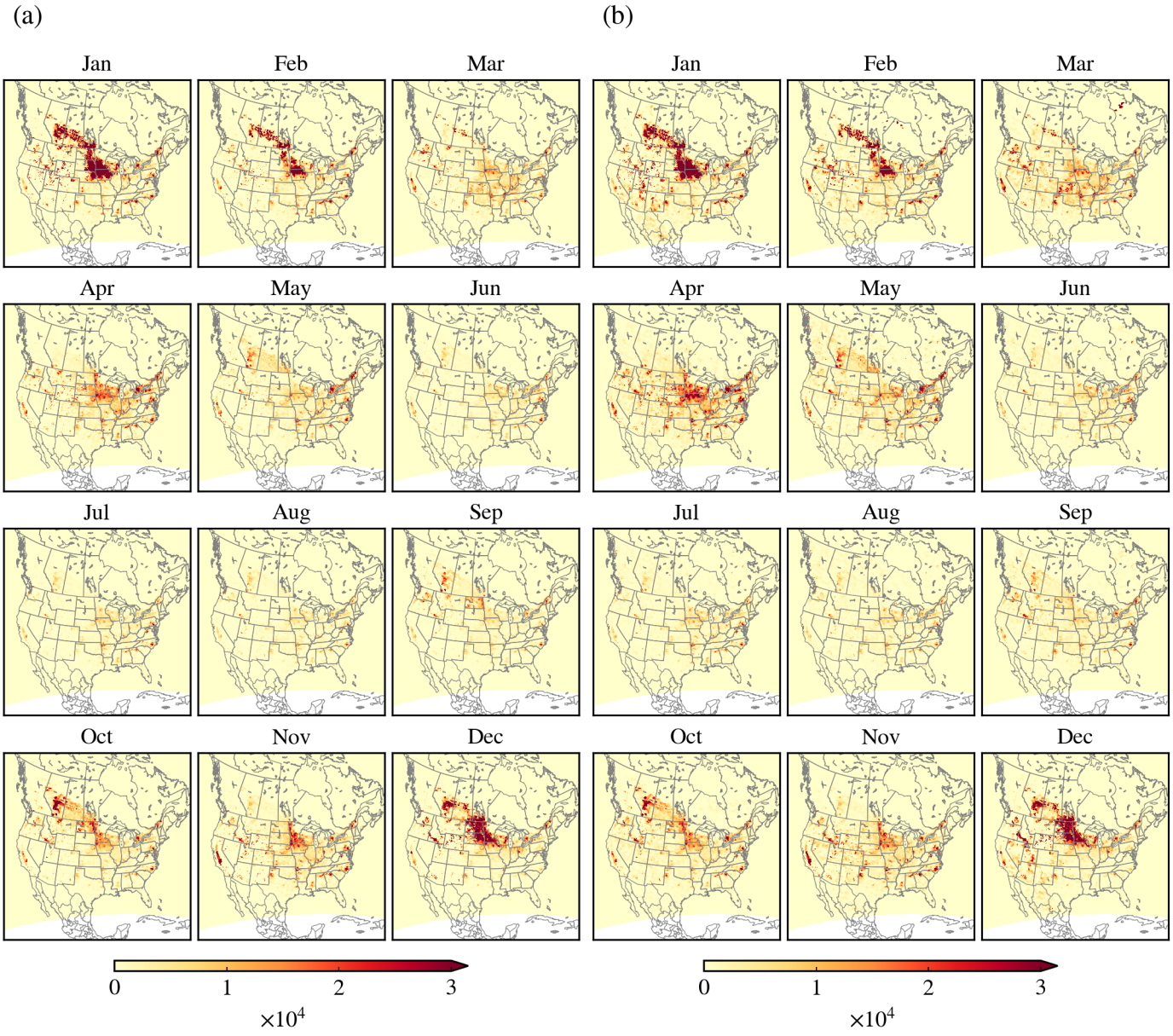

Figure S2. Ammonium potential source Γ_{p} for (a) the background and (b) the analysis.

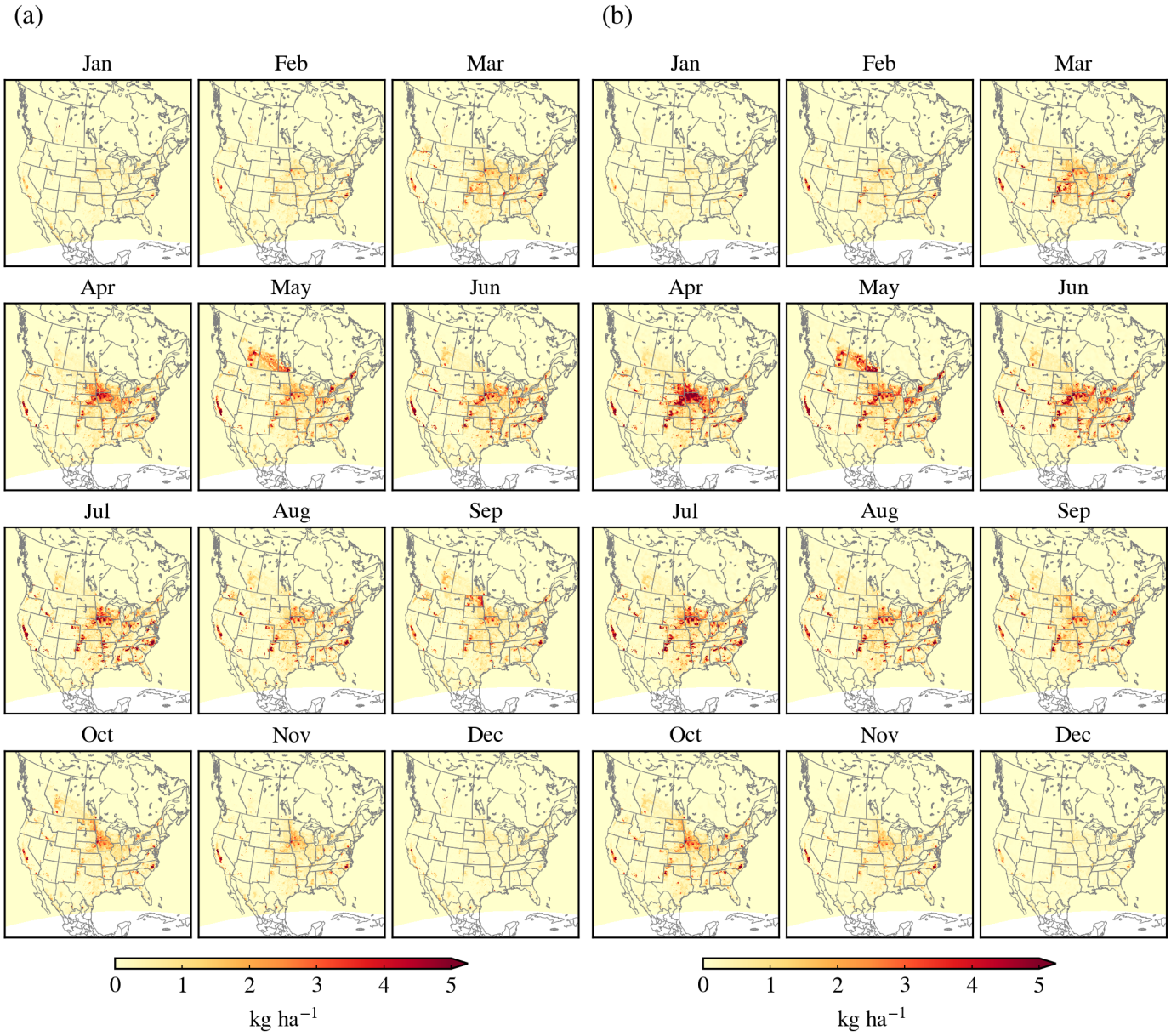

Figure S3. Monthly mean ammonia emissions for (a) the inventory-derived background and (b) the inversions.

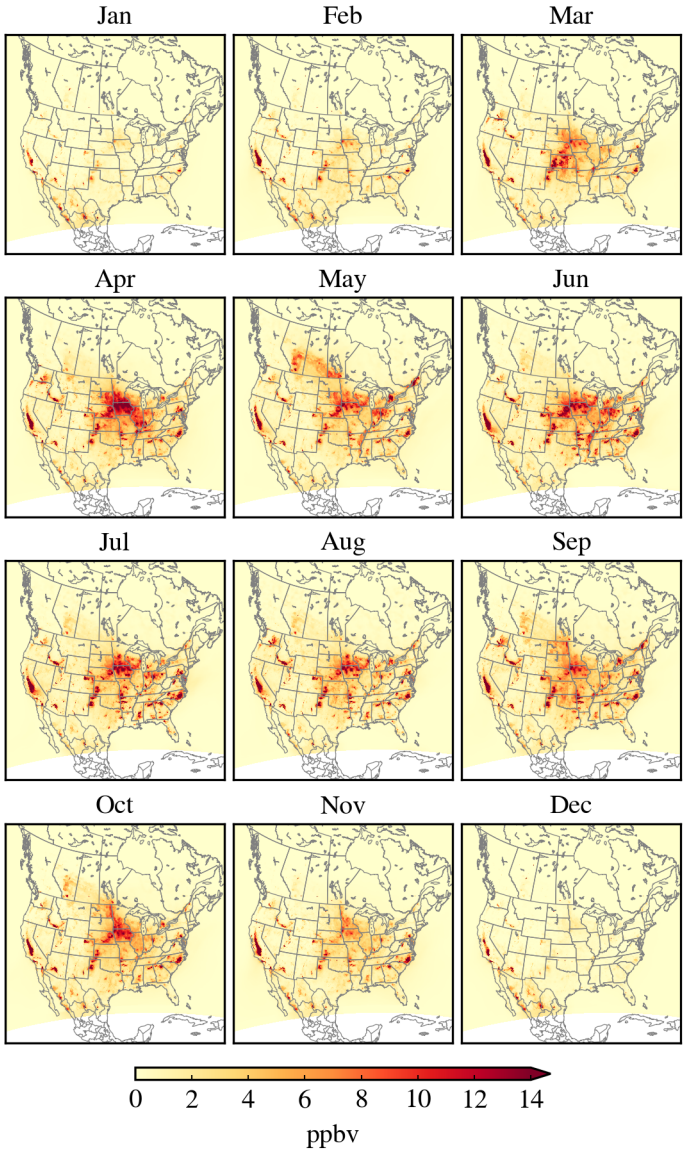

Figure S4. Mean ammonia surface concentrations for the unidirectional flux model using inversion-derived parameters.

month	flux model	bias (%)	STDE (%)	ρ	RMSE (%)
Jan	unidi	-19.3 $\pm$ 4.7	52.6 $\pm$ 3.3	0.55 $\pm$ 0.06	56.0 $\pm$ 3.5
	bidi	-27.4 $\pm$ 4.9 (77)	55.0 $\pm$ 3.5 (38)	0.48 $\pm$ 0.07 (68)	61.4 $\pm$ 3.8 (70)
Feb	unidi	-17.1 $\pm$ 4.5	68.1 $\pm$ 3.2	0.60 $\pm$ 0.04	70.2 $\pm$ 3.3
	bidi	-24.2 $\pm$ 4.6 (73)	69.2 $\pm$ 3.3 (20)	0.55 $\pm$ 0.05 (72)	73.3 $\pm$ 3.4 (49)
Mar	unidi	15.1 $\pm$ 3.1	56.7 $\pm$ 2.2	0.81 $\pm$ 0.02	58.6 $\pm$ 2.2
	bidi	-9.0 $\pm$ 2.8 (100)	51.6 $\pm$ 2.0 (92)	0.80 $\pm$ 0.02 (39)	52.4 $\pm$ 2.0 (96)
Apr	unidi	50.0 $\pm$ 12.8	192.6 $\pm$ 9.1	0.34 $\pm$ 0.06	199.0 $\pm$ 9.3
	bidi	29.2 $\pm$ 11.9 (76)	179.0 $\pm$ 8.4 (73)	0.36 $\pm$ 0.06 (26)	181.4 $\pm$ 8.5 (83)
May	unidi	20.6 $\pm$ 5.1	78.0 $\pm$ 3.6	0.73 $\pm$ 0.03	80.6 $\pm$ 3.7
	bidi	6.8 $\pm$ 4.7 (95)	72.2 $\pm$ 3.4 (76)	0.74 $\pm$ 0.03 (13)	72.5 $\pm$ 3.4 (89)
Jun	unidi	13.0 $\pm$ 6.1	92.9 $\pm$ 4.3	0.74 $\pm$ 0.03	93.8 $\pm$ 4.4
	bidi	-1.4 $\pm$ 5.6 (92)	85.1 $\pm$ 4.0 (82)	0.75 $\pm$ 0.03 (31)	85.2 $\pm$ 4.0 (86)
Jul	unidi	13.7 $\pm$ 7.4	114.7 $\pm$ 5.3	0.58 $\pm$ 0.04	115.5 $\pm$ 5.3
	bidi	-3.6 $\pm$ 6.5 (92)	99.9 $\pm$ 4.6 (97)	0.58 $\pm$ 0.04 (16)	100.0 $\pm$ 4.6 (97)
Aug	unidi	3.3 $\pm$ 5.2	99.3 $\pm$ 3.7	0.64 $\pm$ 0.03	99.3 $\pm$ 3.7
	bidi	-13.3 $\pm$ 4.4 (98)	83.2 $\pm$ 3.1 (100)	0.68 $\pm$ 0.03 (81)	84.3 $\pm$ 3.1 (100)
Sep	unidi	39.1 $\pm$ 6.5	100.3 $\pm$ 4.6	0.64 $\pm$ 0.04	107.6 $\pm$ 4.9
	bidi	13.6 $\pm$ 5.2 (100)	80.0 $\pm$ 3.7 (100)	0.64 $\pm$ 0.04 (6)	81.1 $\pm$ 3.7 (100)
Oct	unidi	27.0 $\pm$ 5.3	79.8 $\pm$ 3.7	0.68 $\pm$ 0.04	84.2 $\pm$ 3.9
	bidi	0.9 $\pm$ 4.0 (100)	61.2 $\pm$ 2.9 (100)	0.72 $\pm$ 0.03 (72)	61.2 $\pm$ 2.9 (100)
Nov	unidi	-12.5 $\pm$ 6.1	94.0 $\pm$ 4.4	0.62 $\pm$ 0.04	94.8 $\pm$ 4.4
	bidi	-32.5 $\pm$ 5.5 (98)	84.3 $\pm$ 3.9 (90)	0.68 $\pm$ 0.04 (89)	90.4 $\pm$ 4.1 (54)
Dec	unidi	-34.9 $\pm$ 4.0	61.5 $\pm$ 2.8	0.48 $\pm$ 0.05	70.7 $\pm$ 3.1
	bidi	-36.5 $\pm$ 4.0 (21)	62.7 $\pm$ 2.9 (23)	0.45 $\pm$ 0.05 (48)	72.5 $\pm$ 3.2 (31)
all	unidi	9.1 $\pm$ 1.8	100.0 $\pm$ 1.3	0.62 $\pm$ 0.01	100.5 $\pm$ 1.3
	bidi	-7.7 $\pm$ 1.6 (100)	89.2 $\pm$ 1.2 (100)	0.64 $\pm$ 0.01 (80)	89.5 $\pm$ 1.2 (100)

Table S1. Comparison statistics using AMoN ammonia surface observations for the unidirectional ('unidi') and bidirectional ('bidi') flux models. Both flux models use inversion-derived parameters. 'all' under the 'month' column indicates statistics taken over the whole year. Numbers in brackets indicate the statistical significance (as a percentage) of the difference between the statistics values for the unidirectional and bidirectional models.

month	flux model	bias (%)	STDE (%)	ρ	RMSE (%)
Jan	unidi	-45.2 ± 21.7	197.3 ± 15.5	0.49 ± 0.08	202.4 ± 15.7
	bidi	-48.3 ± 21.7 (8)	198.1 ± 15.5 (3)	0.50 ± 0.08 (7)	203.9 ± 15.9 (5)
Feb	unidi	-10.9 ± 10.2	99.5 ± 7.3	0.38 ± 0.09	100.1 ± 7.3
	bidi	-13.2 ± 10.4 (13)	101.2 ± 7.4 (13)	0.35 ± 0.09 (27)	102.0 ± 7.4 (15)
Mar	unidi	-58.1 ± 27.1	229.6 ± 19.4	0.79 ± 0.05	236.9 ± 19.8
	bidi	-65.8 ± 30.4 (15)	257.6 ± 21.7 (66)	0.68 ± 0.07 (96)	265.8 ± 22.2 (67)
Apr	unidi	-4.2 ± 19.5	175.1 ± 13.9	0.67 ± 0.06	175.2 ± 13.8
	bidi	-14.2 ± 20.3 (28)	182.3 ± 14.5 (28)	0.64 ± 0.07 (41)	182.9 ± 14.4 (30)
May	unidi	23.6 ± 17.4	170.1 ± 12.4	0.63 ± 0.06	171.7 ± 12.5
	bidi	18.5 ± 18.9 (16)	183.9 ± 13.4 (55)	0.55 ± 0.07 (81)	184.8 ± 13.4 (52)
Jun	unidi	-21.9 ± 21.4	202.8 ± 15.2	0.54 ± 0.08	204.0 ± 15.2
	bidi	-21.7 ± 17.7 (1)	167.6 ± 12.6 (93)	0.71 ± 0.05 (99)	169.0 ± 12.6 (92)
Jul	unidi	-13.9 ± 8.0	82.4 ± 5.7	0.79 ± 0.04	83.6 ± 5.8
	bidi	-14.5 ± 7.4 (5)	76.2 ± 5.3 (58)	0.83 ± 0.03 (68)	77.5 ± 5.3 (56)
Aug	unidi	-3.2 ± 21.5	206.4 ± 15.3	0.36 ± 0.09	206.4 ± 15.3
	bidi	-17.2 ± 20.8 (36)	199.4 ± 14.8 (25)	0.36 ± 0.09 (1)	200.2 ± 14.8 (23)
Sep	unidi	-2.7 ± 15.8	147.0 ± 11.2	0.76 ± 0.05	147.1 ± 11.2
	bidi	-11.2 ± 16.8 (28)	157.1 ± 12.0 (46)	0.72 ± 0.05 (61)	157.5 ± 12.0 (48)
Oct	unidi	1.9 ± 16.6	162.6 ± 11.8	0.38 ± 0.09	162.6 ± 11.8
	bidi	-6.7 ± 15.6 (29)	152.9 ± 11.1 (45)	0.43 ± 0.08 (41)	153.1 ± 11.1 (44)
Nov	unidi	-27.7 ± 9.7	91.5 ± 6.9	0.47 ± 0.08	95.5 ± 7.2
	bidi	-32.2 ± 9.0 (27)	85.1 ± 6.4 (50)	0.53 ± 0.08 (54)	91.0 ± 6.8 (35)
Dec	unidi	-8.6 ± 7.3	71.1 ± 5.2	0.42 ± 0.09	71.7 ± 5.2
	bidi	-13.0 ± 7.5 (32)	72.6 ± 5.3 (16)	0.36 ± 0.09 (50)	73.8 ± 5.4 (22)
all	unidi	-13.1 ± 4.8	159.1 ± 3.4	0.57 ± 0.02	159.6 ± 3.4
	bidi	-18.7 ± 4.8 (59)	159.2 ± 3.4 (2)	0.56 ± 0.02 (23)	160.3 ± 3.4 (11)

Table S2. Same as Table S1 but for NAPS.

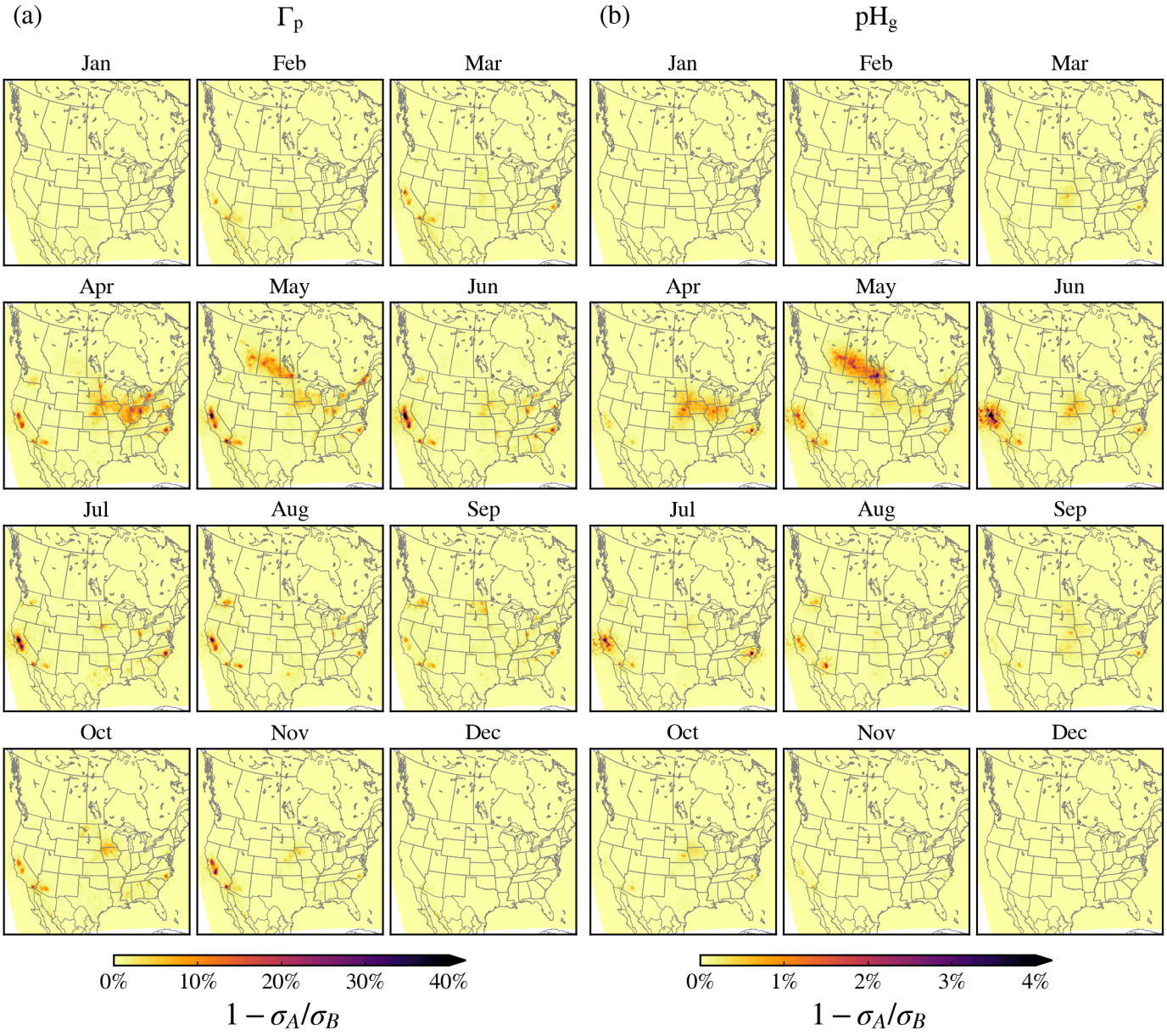

Figure S5. Reduction of the analysis (a posterior) uncertainties σ_A relative to the background (a priori) uncertainties σ_B for the inversion parameters (a) Γ_p and (b) pH_g.

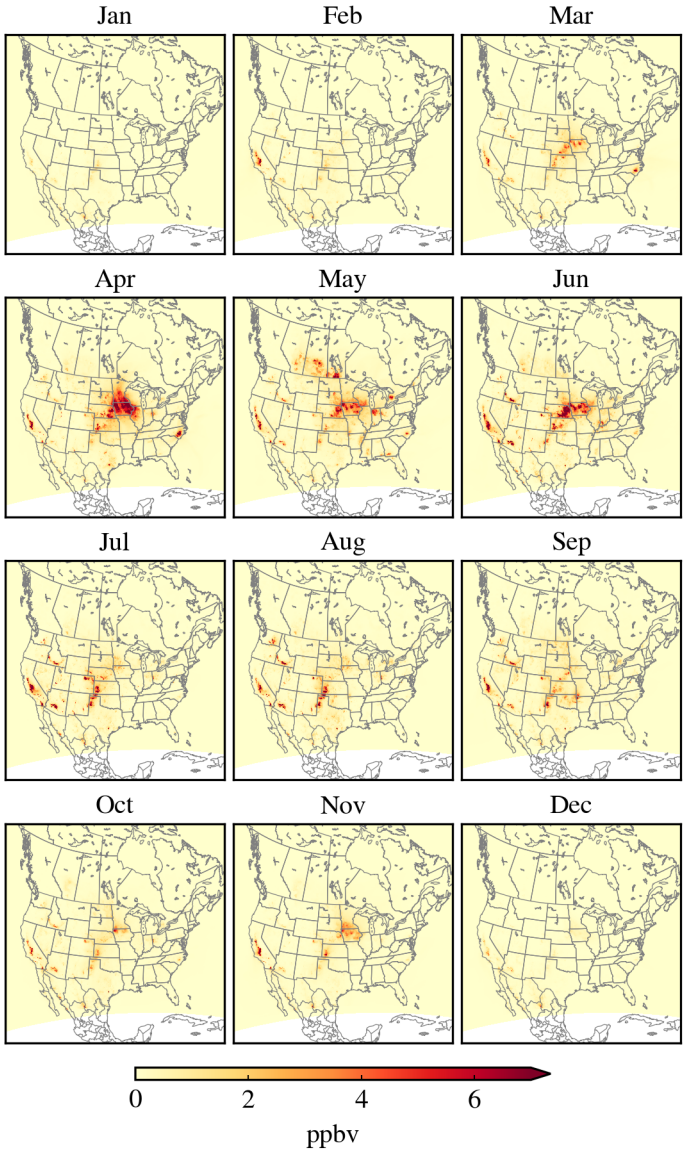

Figure S6. Root mean square differences in ammonia surface concentrations between bidirectional flux models. The first bidirectional flux model has both Γ_{p} and $\mathrm{pH_g}$ derived from inversions. The second bidirectional flux model has only Γ_{p} inversion-derived and $\mathrm{pH_g}$ set from values from the WoSIS pH database.

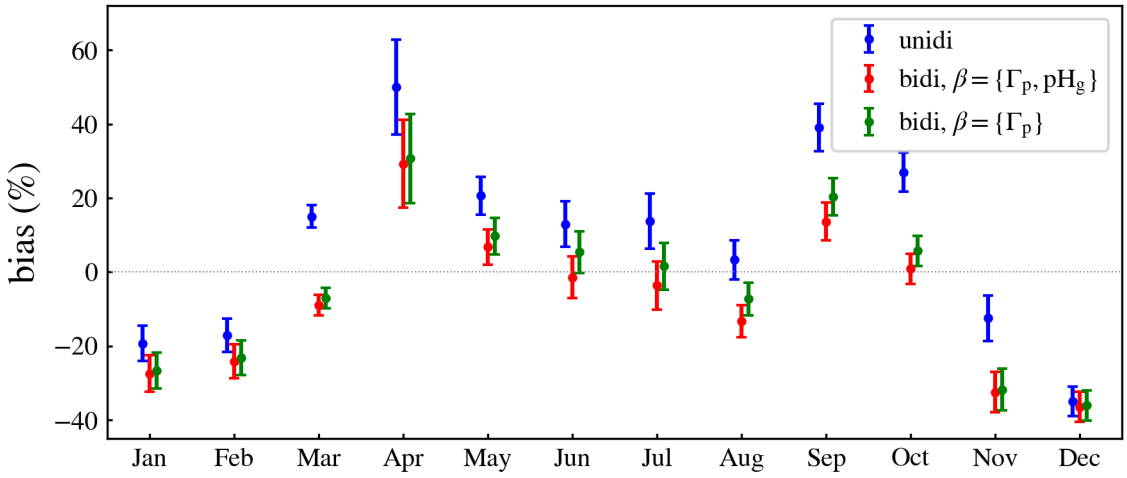

Figure S7. Biases of the unidirectional model (with inversion-derived emissions; blue), the bidirectional flux model with both Γ_p and pH_g set from inversions (red), and the bidirectional flux model with only Γ_p set from inversions and pH_g set from values from the WoSIS pH database (green) as compared to AMoN observations for 2016. Error bars indicate the 1σ confidence interval.